Pergamon

Bioorganic & Medicinal Chemistry 8 (2000) 2663–2673

BIOORGANIC & MEDICINAL CHEMISTRY

3-D QSAR Analysis of Inhibition of Murine Soluble Epoxide Hydrolase (MsEH) by Benzoylureas, Arylureas, and their Analogues

Yoshiaki Nakagawa,[a,*] Craig E. Wheelock,[a,b] Christophe Morisseau,[b] Marvin H. Goodrow,[b] Bruce G. Hammock[b] and Bruce D. Hammock[b]

[a]*Division of Applied Life Sciences, Graduate School of Agriculture, Kyoto University, Kyoto 606-8502, Japan*
[b]*Department of Entomology, University of California, Davis, CA 95616, USA*

Received 1 June 2000; accepted 18 July 2000

Abstract—Two hundred and seventy-one compounds including benzoylureas, arylureas and related compounds were assayed using recombinant murine soluble epoxide hydrolase (MsEH) produced from a baculovirus expression system. Among all the insect growth regulators assayed, 18 benzoylphenylurea congeners showed weak activity against MsEH. Newly synthesized cyclohexylphenylurea, 1-benzyl-3-phenylurea, and 1,3-dibenzylurea analogues were rather potent. The introduction of a methyl group at the *para*-position of the phenyl ring of cyclohexylphenylurea enhanced the activity 6-fold, though similar substituent effects were not seen for any of the benzoylphenylureas. The activities of these compounds, including several previously reported compounds, such as dicyclohexylurea, diphenylurea, and their related analogues (Morisseau et al., *Proc. Natl. Acad. Sci.*, **1999**, *96*, 8849), were quantitatively analyzed using comparative molecular field analysis (CoMFA), a three-dimensional quantitative structure–activity relationship (3-D QSAR) method. Both steric and electrostatic factors contributing to variations in the activity were visualized using CoMFA. CoMFA results showed that one side of the cyclohexylurea moiety having a *trans*-amide conformation (A-ring moiety) is surrounded by large sterically unfavorable fields, while the other side of A-ring moiety and the other cyclohexyl group (B-ring moiety) is encompassed by sterically favored fields. Electrostatically negative fields were scattered around the entire molecule, and a positive field surrounds the carbon of the carbonyl group. Hydrophobic fields were visualized using Kellogg's hydropathic interaction (HINT) in conjunction with CoMFA. Hydrophobically favorable fields appeared beside the 4- and 4′-carbon atoms of the cyclohexyl groups, and hydrophobically unfavorable fields surrounded the urea bridge. The addition of the molecular hydrophobicity, it > /it >, to CoMFA did not improve the correlation significantly. The ligand-binding interactions shown by X-ray crystallographic data were rationalized using the results of the CoMFA and HINT analyses, and the essential physicochemical parameters for the design of new MsEH inhibitors were disclosed.

Introduction

Epoxide hydrolases (EHs, EC 3.2.2.3) are found in both animals and plants, and play a role in regulating the metabolism of hormones and secondary metabolites in biological systems.[1–3] Among various EHs, microsomal EH (mEH) and soluble EH (sEH) are particularly important enzymes due to their ability to detoxify mutagenic, toxic, and carcinogenic xenobiotic epoxides.[1,2] In addition mEH has been hypothesized to have an endogenous role in bile acid transport,[4,5] while sEH is potentially involved in the metabolism of oxidized lipids as autacoids or chemical mediators.[6]

We have shown that leukotoxin (linoleic acid epoxide) is not directly cytotoxic to cells, but that the diol metabolite is toxic in all cells assayed to date, including pulmonary alveolar epithelia cells.[6] Therefore, powerful and selective inhibitors of sEH could be useful for studying sEH as pharmaceutical target. To increase our understanding of this enzyme, we have recently determined the X-ray structure of inhibitor bound murine sEH (MsEH) and proposed an inhibitory mechanism of action.[7,8] To further extend our knowledge of this enzyme, it is

Abbreviations: CPU, *N*-cyclohexyl-*N*′-(3-phenyl)propylurea; CIU, *N*-cyclohexyl-*N*′-(4-iodophenyl)urea; CDU, *N*-cyclohexyl-*N*′-decylurea; CoMFA, comparative molecular field analysis; CoMSIA, comparative similarity indices analysis; 3-D QSAR, three-dimensional quantitative structure–activity relationship; DCU, dicyclohexylurea; HINT, hydropathic interaction; MsEH, murine soluble epoxide hydrolase; SAR, structure–activity relationship.

*Corresponding author. Tel.: +81-75-753-6117; fax: +81-75-753-6123; e-mail: naka@kais.kyoto-u.ac.jp

0968-0896/00/$ - see front matter
PII: S0968-0896(00)00198-X

important to model the essential physicochemical factors involved for inhibitors which demonstrate high activity. These factors are not only necessary for the basic understanding of the inhibitory mechanism, but also for the design of more potent inhibitors.

Recent studies have shown chalcone oxides (**I**; Fig. 1) to be potent inhibitors of sEH.[9] These compounds contain a carbonyl group beta to the epoxide and essentially act as poor substrates, thus their ability to inhibit the enzyme. However, we have found that dicylohexylurea (DCU, **II**; Figure 1) and several urea and carbamate analogues were much more potent inhibitors of sEH. This group of inhibitors acts through a transition state analogue mechanism with Asp333 in the sEH active site attacking the carbonyl carbon of the urea moiety. We therefore combined the components of the 2 active groups of inhibitors to test benzoylphenylureas (**III**; Figure 1) as inhibitors. This class of compounds contains the potent urea moiety as well as the carbonyl group beta to the site of nucleophilic attack as in the chalcone oxides.

In addition to the benzoylphenylureas, several of these compounds have commercial applications, with urea and carbamate moieties being very common in pesticides and medicines. Several urea containing pesticides have been shown to be potent inhibitors, including diuron and siduron,[10] as well as the carbamates such as phenoxycarb and carbaryl. It is therefore important to have an understanding of how these compounds interact with their enzymatic target. Benzoylphenylureas and related compounds are well-known chitin synthesis inhibitors in insects,[11–13] and some of them have applications for agricultural use. These compounds can also be used in the dairy industry for controlling flies and mosquitoes. Although benzoylphenylureas inhibit chitin synthesis, they have no effect on insect chitin synthase.[11–13] Diflubenzuron, a benzoylphenylurea, elicited several effects in cell free systems: inhibition of calcium uptake[14] and the activation of protein phosphorylation[15,16] in a cell-free preparation of the American cockroach (*Periplaneta americana*), inhibition of chitin synthase in brine shrimp,[17] and activation of serine proteases.[18] Many hypotheses have been proposed regarding the mode of action of benzoylphenylureas; however, the actual mechanism remains unknown.[19,20] In addition, some benzoylphenylurea congeners showed antitumor activity,[21,22] antimitotic effects,[23,24] and the stimulation of hematopoesis.[25]

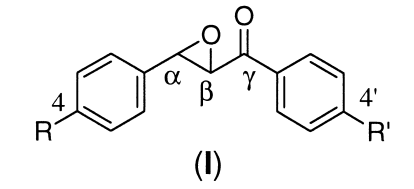

(I)

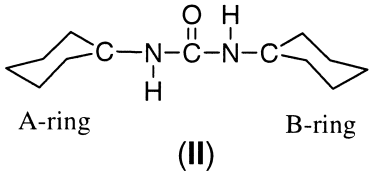

(II)

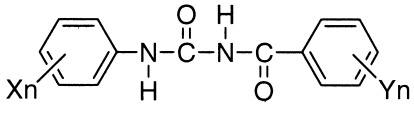

(III)

Figure 1. Structures of chalcone oxides (**I**), DCU (**II**), and benzoylphenylureas (**III**) derived from the X-ray structure of diflubenzuron obtained from the Cambridge data base.

The aim of this study was 3-fold. The first aim was to determine the effect of these insect growth regulators on MsEH, since they contain the essential components for inhibitory activity. The second aim was to examine the structure–activity relationship (SAR) for the inhibition of MsEH by several ureas, carbamates, and their analogues. Thirdly, we wanted to visualize the ligand–enzyme interactions using computer graphics techniques in the hope of being able to predict the essential qualities necessary for the synthesis of more potent inhibitors. Essential physicochemical properties were extracted, including electrostatic, steric, and hydrophobic interactions. We used comparative molecular field analysis (CoMFA),[26] a three-dimensional quantitative structure–activity relationship (3-D QSAR) technique, as well as CoMFA combined with hydropathic interaction (HINT) analysis,[27] to model the key interactions of MsEH. Enzyme assays were performed using recombinant MsEH produced in a baculovirus expression system as previously reported.[9,28,29] Using this CoMFA model we can predict compound activity, and design potent sEH inhibitors, thereby increasing our understanding of the enzyme as well as developing new tools for use as a potential pharmaceutical target.

Minimized conformations and superpositions between compounds

Modeling and calculation experiments were executed using SYBYL (ver. 6.5.3; Tripos Co., St. Louis, MO, USA). The X-ray crystallographic coordinates of 1-(4-chlorophenyl)-3-(2,6-difluorobenzoyl)urea (**18**, diflubenzuron)[30] were applied in the construction of the initial conformations of the urea derivatives and related compounds. The X-ray data were downloaded from Cambridge data base, and the benzoylphenylurea basic structure is sketched as shown in structure **III** of Figure 1. The phenyl moiety of benzoylphenylurea is attached to the *trans*-amide moiety and the benzoyl group to the *cis*-amide.

The structures of DCU (**35**) and diphenylurea (**44**) were constructed by replacing the benzoyl and phenyl groups of diflubenzuron (**18**) with the corresponding cyclohexyl or phenyl groups. To distinguish the two cyclohexyl

groups of DCU the cyclohexyl group attached to the *trans*-amide is labeled as the A-ring, and the other cyclohexyl group as the B-ring, as shown in structure **II** of Figure 1. The most favorable torsion angles for the -C(Ar)-C(Ar)-N-H portion at the aniline moiety (C_6H_5-NH-) of diphenylurea (**44**) and the corresponding cyclohexyl moiety (C_6H_{11}-NH-) of dicyclohexylurea (**35**) were determined by executing a Grid Search procedure, a SYBYL submodule which systematically searches and minimizes every conformation using molecular mechanics (MM2). The search was performed with an increment of 30 degrees, thus producing 12 conformers from which the energetically minimized conformation had to be determined. The structure of compound **34** was built from compound **35**. Other dicyclohexyl analogues (**36**–**39**) were constructed by changing the nitrogen or oxygen atom of compound **35** to the corresponding atom. Compounds **16**, **17** and **40**–**43** were constructed from compound **35** by replacing the cyclohexyl group with the corresponding moieties. Compound **45** was derived from compound **44** by replacing both N atoms with C atoms, and compound **46** was constructed from compound **45** by substituting a C atom with an O atom. Compounds **49** and **50** were constructed by attaching the necessary CH_3 group to compound **44**. The most favorable torsion angle between the OPh group and the phenyl ring of compounds **2**, **3**, and **22** was determined using a Grid Search as described above. The final conformations and the atomic charges of all compounds were minimized by the semi-empirical molecular orbital methods PM3 and MNDO, respectively. According to the X-ray structures of *N*-cyclohexyl-*N*′-(3-phenyl)propylurea (CPU),[7] *N*-cyclohexyl-*N*′-decylurea (CDU) and *N*-cyclohexyl-*N*′-(4-iodophenyl)urea (CIU)[8] each cyclohexyl group is attached to the *trans*-amide corresponding to the A-ring in structure **II** (Fig. 1). Therefore, the cyclohexyl groups of compounds **4**, **5**, **16**, **17**, **40**, **42**, **43** and **51** were placed as the A-ring.

DCU (**35**) was used as a template for the superposition of other related compounds using from 5 to 8 atoms and a root mean square (RMS) fitting method. All structures were superimposed as displayed in Tables 1–3, in which fitting atoms are shown in bold type. In most cases the 8 atoms of the urea moiety (-C-NH-CO-NH-C-) were used for the superposition. In cases where there was no common fitting N atom (**36**–**38**, **45**–**48**), the corresponding carbon or hetero atom was used. For compounds **34**, **36**–**38**, **45**–**47**, **49**, **50** and **52**, an H atom was not used in the superpositions due to the lack of an -NH hydrogen atom. In the case of the thiourea analogues in compounds **13**–**15** and **39**, an S atom was used instead of an O atom for the superposition.

HINT–CoMFA

The analyses were carried out using the QSAR module of SYBYL 6.5.3 and HINT 2.30S (eduSoft, Ashland, VA, USA). The lattice spacing was 2 Å, a +1 charge was used to estimate the electrostatic field, and an sp^3 carbon was used to estimate the steric molecular fields. The required region to accommodate the structures which were superposed according to the above scheme was automatically prepared in the CoMFA module. The electrostatic and steric potential energies at each lattice point were calculated using Coulombic and Lennard-Jones potential functions, respectively. The hydrophobic effects were examined using either HINT terms or it> /it> values as an additional independent variable. The default setting was used for the calculation of CoMFA and HINT lattice variables. The correlations of the biological activity index with the lattice variables and it> /it> were analyzed by the partial least squares (PLS) method with a column filtering setting of 2 kcal mol^{-1}. The CoMFA results were represented by the predictive r^2 value which was renamed as q^2,[31] and standard errors of cross-validated predictions, s_{press}, as well as the number of optimum components, m, from the leave-one-out cross-validation analyses. In addition the conventional correlation coefficient, r, standard deviation, s, and the weight percentage of the type of the descriptors participating in the correlation were produced from the analysis. The results were visualized by color contour maps, which display both the favorable and unfavorable fields for each electrostatic, steric and hydrophobic interaction surrounding a set of superposed molecules.

Results

Inhibition of sEH

Two hundred and seventy-one substituted benzoylphenylurea analogues including 2,6-difluorobenzoyl, 2,6-dichlorobenzoyl, and 4-chlorophenyl analogues, and related compounds including thiadiazoles, oxalyldianilides, *N,N*-dimethyl phenyl carbamates, and dibenzoylhydrazines were assayed against MsEH. Among the compounds tested, only 18 benzoylphenylureas (**18**–**33**) were significant inhibitors of MsEH. Their pIC_{50} values are listed in Table 2, although their activity is only about 1/1000 that of the potent inhibitors DCU (**35**) and dicyclohexylcarbamate (**36**). As shown in Table 2, highly pure diflubenzuron (**18**) synthesized for this study and purified through repeated crystallizations was inactive ($pIC_{50} < 4.00$); however, the industrial grade obtained from a company demonstrated some activity ($pIC_{50} = 4.57$), indicating the presence of unknown contaminant(s). Other acylurea analogues tested did not give 50% inhibition, even at concentrations up to 100 μM.

Newly synthesized benzoylureas (**1**–**9**), having substituted phenyl, cyclohexyl, cyclododecyl, or benzyl groups as the aniline moiety, were inactive. However, three compounds **10**–**12** containing benzyl groups in place of the benzoyl group were active inhibitors. Two benzylphenylureas (**10** and **11**) were equipotent to diphenylurea (**44**), and a dibenzylurea (**12**) was slightly lower. By replacing a phenyl group of diphenylurea with a cyclohexyl group, the activity was enhanced three-fold (**16** versus **44**). Furthermore, the introduction of a CH_3 group at the *para*-position of the benzene ring increased the activity about 5 times. Three benzoylthioureas (**13**–**15**) demonstrated some activity.

Table 1. Observed and calculated pIC_{50} values for inhibition of MsEH by newly synthesized benzoylureas, benzylureas, and phenylureas

No.	Structure[a]	pIC_{50} (M) Obsd.	pIC_{50} (M) Calcd[b]	log*P*[c]	HINT log*P*[d]
1	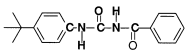	< 4.00	4.51	5.22	12.74
2	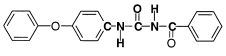	< 4.00	4.22	5.48	12.92
3	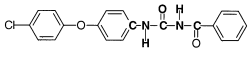	< 4.00	3.97	6.39	13.63
4	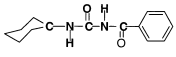	< 4.00	5.82	3.30	4.82
5	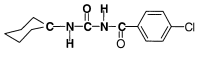	< 4.00	6.05	4.22	5.53
6	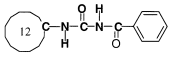	< 4.00	5.17	3.93	7.79
7	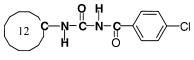	< 4.00	4.94	4.84	8.38
8	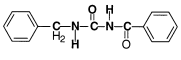	< 4.00	4.98	3.04	4.20
9	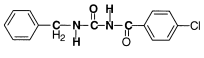	< 4.00	5.03	3.95	4.79
10	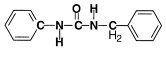	5.62	5.52 (5.53)	2.87	3.54
11	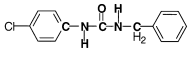	5.74	5.33 (5.75)	3.88	4.13
12	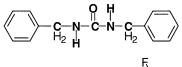	5.27	5.37 (5.20)	2.79	1.55
13	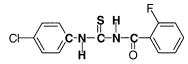	4.06	4.35	3.37	11.14
14	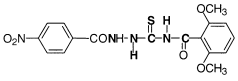	4.34	4.24	1.34	11.14
15	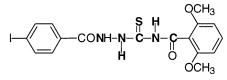	4.31	4.03	2.72	11.33
16	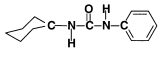	6.12	6.53 (6.19)	3.13	4.16
17	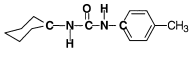	6.89	6.75 (6.80)	3.63	4.82

[a]Fitting atoms used for superpositions are drawn as bold type in each structure.
[b]Calculated by eqn (1) in Table 4. Values in parentheses were calculated by eqn (5) in Table 4.
[c]Empirically estimated from the analogous compounds according to our previous publications (refs 44, 48–50).
[d]Calculated by HINT program developed by Kellogg et al. (ref 27).

3-D QSAR

All compounds with $pIC_{50} < 4.00$ were not included in the QSAR analyses due to the lack of their activity in terms of pIC_{50}. In the following QSAR analyses compound **39** was not included, because it deviated dramatically from the correlation equation. Equation (1) in Table 4 was obtained from the CoMFA analysis of 37 compounds (Tables 1–3). The alignments of the 37 compounds used to derive eqn (1) are shown in Figure 2. In order to assess the role of hydrophobicity, CoMFA analyses were executed with the addition of the molecular hydrophobicity parameter log*P*, giving eqn (2) or (3). However, this addition did not significantly improve the correlation as shown in Table 4. Equation (3) was formulated using 6 components (*m*), because the optimum component number was determined to be 6 in the cross-validation analysis. The calculated activity values from eqn (1) are listed in Tables 1–3 and the relationship between observed pIC_{50} values and calculated values is depicted in Figure 3. Figure 4 shows the overlay of diflubenzuron (**18**) and DCU (**35**) in magenta with the major CoMFA steric and electrostatic potential contour maps, drawn according to eqn (1). The green areas in Figure 4(a) indicate fields where submolecular bulk is well accommodated with an increase in the activity, whereas the yellow indicates fields where the submolecular bulk is unfavorable for activity. The red areas in Figure 4(b) indicate fields where negative electrostatic interaction with the receptor binding site increases the activity, whereas the blue areas show fields where the opposite is the case.

Table 2. Observed and calculated pIC_{50} values for inhibition of MsEH by benzoylphenylureas and their log*P* values.

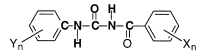

No.	Y_n	X_n	pIC_{50} (M) Obsd.	Eqn (1)	log*P*	HINT log*P*
18	4-Cl	2,6-F_2	< 4.00[a]	4.34	3.88[b]	11.47
19	4-*n*-C_3H_7	2,6-F_2	4.24	4.23	4.34[c]	12.50
20	4-*n*-C_4H_9	2,6-F_2	4.32	4.23	4.86[c]	13.04
21	4-*n*-C_8H_{17}	2,6-F_2	4.11	4.33	6.85[c]	15.20
22	4-OC_6H_5	2,6-F_2	4.06	4.02	4.93[c]	13.08
23	4-CN	2,6-F_2	4.25	4.26	3.06[c]	10.31
24	4-C_6H_5	2,6-F_2	4.14	4.03	4.83[c]	12.75
25	4-Cl	2-$N(CH_3)_2$	4.18	3.87	4.25[c]	11.26
26	4-*n*-C_3H_7	2,6-Cl_2	3.93	4.15	4.86[c]	13.64
27	4-*n*-C_4H_9	2,6-Cl_2	4.04	4.17	5.38[c]	14.18
28	4-*n*-C_6H_{13}	2,6-Cl_2	4.68	4.40	6.37[c]	15.26
29	4-OC_2H_5	2,6-Cl_2	4.07	3.98	3.27[c]	12.49
30	4-$SO_2N(C_2H_5)_2$	2,6-Cl_2	4.37	4.19	4.36[d]	6.90
31	4-$SO_2N(CH_2)_4$	2,6-Cl_2	4.12	4.19	3.60[d]	7.09
32	2-Cl	2,6-Cl_2	4.15	4.57	3.64[d]	12.61
33	2-NO_2	2,6-Cl_2	4.17	4.41	3.30[d]	12.61

[a]The value evaluated for industrial grade of compound (TH-6040) is 4.57.
[b]Experimentally measured in the shake-flask method (ref 48).
[c]Cited from ref 44.
[d]Newly estimated according to the empirical method (refs 49 and 50).

As drawn in Figure 4(a), the large sterically unfavorable fields (yellow areas) are found above the A-ring and urea bridge moiety, whereas three green fields showing the sterically favorable fields are located around the A-ring and an additional field is located beside the cyclohexyl group of the B-ring. In Figure 4(b), negative electrostatic-potential fields (red areas) are spread around the whole molecule and a positive field (blue area) is found below the carbonyl carbon atom in the urea moiety.

In order to visualize the partial hydrophobic fields in the CoMFA analysis, we used the HINT procedure[27] along with CoMFA.[26] The polar proximity used for

Table 3. Observed and calculated pIC_{50} values for ureas and their analogues, and their log*P* values

No.	Structures[a]	pIC50 Obsd.	pIC50 Calcd[b]	log*P*	HINT log*P*
34	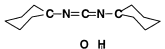	6.60	6.66 (6.75)	4.38	2.70
35	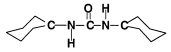	7.05	6.95 (7.11)	3.51	2.91
36	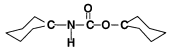	7.30	6.77 (7.05)	3.90	3.64
37	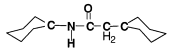	6.24	6.66 (6.34)	3.60	3.77
38	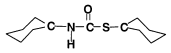	5.42	5.89	4.69	3.78
39	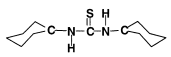	4.00[c]	6.77	3.79	3.45
40	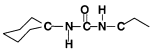	5.80	6.30 (5.81)	2.54	1.82
41	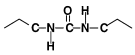	< 3.30	5.70 (4.50)	1.57	0.61
42	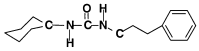	7.22	7.05 (7.12)	3.96	3.37
43	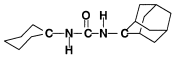	7.22	6.96 (7.34)	4.14	3.63
44	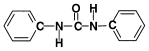	5.64	5.61	3.00	11.52
45	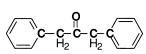	3.37	3.33 (3.31)	3.13	2.86
46	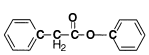	3.37	3.17 (3.40)	3.34	4.68
47	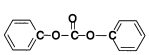	< 3.30	4.47	3.28	3.63
48	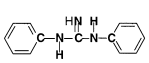	< 3.30	4.12	−0.05	2.50
49	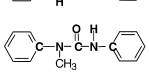	3.71	3.96	2.75	10.33
50	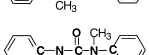	< 3.30	3.94	3.20	9.02
51	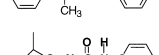	6.80	6.44 (6.84)	3.65	4.60
52	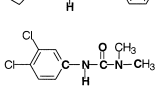	3.91	3.96 (3.99)	2.68	3.88

[a]Fitting atoms used for superpositions are drawn as bold type in each structure.
[b]Calculated by eqn (1) in Table 4. Values in parentheses were calculated by eqn (5) in Table 4.
[c]This value is not included in the QSAR analysis.

the calculation of HINT lattice variables was calculated using the option "Via Bond", which was performed by the Leo–Hansch method of log*P* calculation.[32,33] However, some log*P* values calculated using HINT were significantly different from the experimentally/empirically measured log*P* values or resulted in warning messages following the HINT calculation. We therefore omitted these 21 compounds (**13**–**15**, **19**–**33**, **38**, **44**, **49**) from the compound set for eqn (1) in the HINT–CoMFA analysis. Equation (4) was derived for this small set of compounds ($n=16$), and the quality in the cross-validation analysis was worse than that of eqn (1). The steric and electrostatic fields obtained for this small set of compounds ($n=16$) are not greatly different from that obtained for the 37 compounds in eqn (1). CoMFA–HINT analysis was performed for this small set of compounds to derive eqn (5), and the hydrophobic fields are visualized in Figure 4(c). The hydrophobically favorable fields (orange areas) are found around both cyclohexyl moieties, and hydrophobically unfavorable fields (cyan blue areas) are located around the urea bridge.

All compounds except for compound **39** were well predicted ($r^2=0.955$) by eqn (1), as shown in Figure 3. If compound **39** was included in the CoMFA analysis the conventional correlation was poor (cross-validated $q^2=0.567$, $s_{press}=0.837$, $m=3$, $r^2=0.873$, $s=0.454$, $F=77.601$). The activity of the benzoylphenylureas (**18**–**33**) listed in Table 2, as well as the newly synthesized inactive benzoylphenylureas (**1**–**3**), was roughly predicted by this QSAR model. However, newly synthesized benzoylureas (**4**–**7**) were not rationalized by this current mode. Previously reported inactive compounds **47**, **48** and **50**[9] were also predicted to have low activity, having similar potency as the benzoylphenylureas, while compound **41** was not predicted. The use of additional compounds should serve to increase the accuracy of this equation. Although the cyclohexyl group for compounds **4** and **5** was placed on the left hand side (A-ring moiety) in the superposition, it may flip, resulting in the placement of the cyclohexyl group on the right (B-ring).

According to our unpublished data, most of the thiourea analogues had very little or no activity, but three thiourea analogues (**13–15**) were reasonably included in eqn (1). The activity of compound **39** having a C=S group was predicted to be rather high (6.77), being similar to that (7.05) of DCU (**35**) however; the observed activity was 4.00. Compounds **14** and **15** were utilized to synthesize the thiadiazole analogues whose

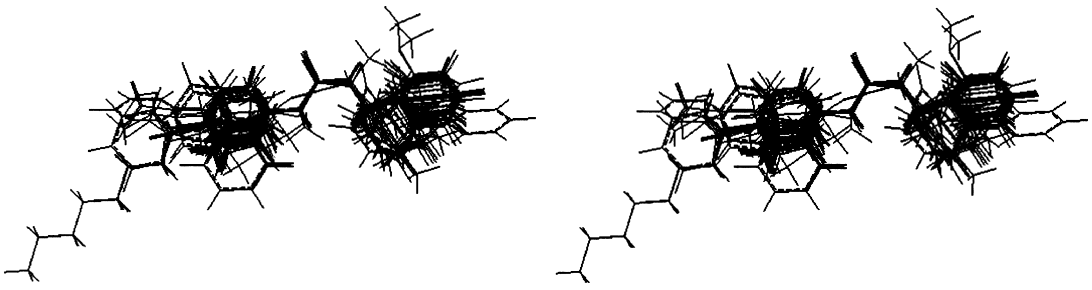

Figure 2. The superposition of the 37 compounds used for the CoMFA analysis.

Table 4. CoMFA correlation statistics for two compounds set ($n = 16$ and 37)

Cross-validation			Conventional correlation				Contribution (%)[a]			
N	q^2	s_{press}	m	r^2	s	F	EL	ST	H	Eqn
37	0.750	0.650	4	0.955	0.275	170.724	42.6	57.4	—	1
37	0.726	0.680	4	0.930	0.345	105.695	40.3	55.6	4.1[b]	2
37	0.745	0.678	6	0.968	0.371	90.234	41.4	53.2	5.4[b]	3
16	0.634	0.938	4	0.983	0.200	163.406	32.6	67.4	—	4
16	0.636	0.982	5	0.994	0.126	330.981	22.6	42.2	35.2	5

[a]Contribution of electronic (EL), steric (ST), and hydrophobic effects (H) in the calculation.
[b]Molecular hydrophobicity log$P$ was used as the independent parameter in the analysis.

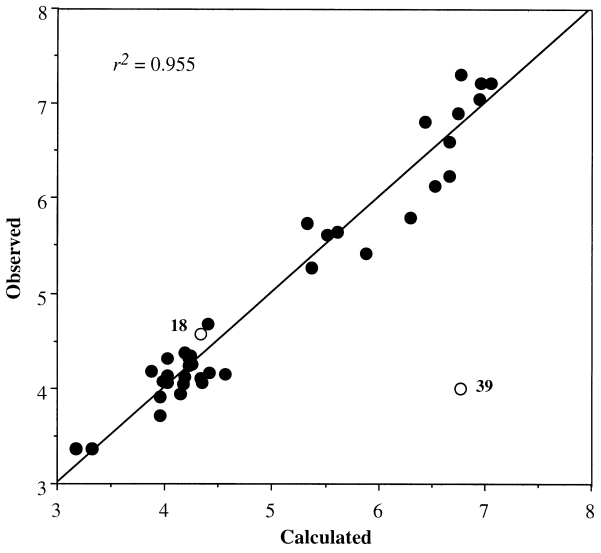

Figure 3. Plot of observed activity values for inhibition of murine sEH versus the calculated values using eqn (1). All values are shown to inhibit 50% of the enzyme (IC_{50}). (●) Indicates compounds included in the correlation analysis ($n = 37$); (○) indicates excluded compounds (industrial grade of diflubenzuron **18** and a thiourea **39**).

mode of action is similar to that of benzoylphenylureas.[34] Although 16 thiadiazole analogues with various substituents at both benzene rings were assayed, none of them were active. These results suggest that metabolites which are derived by the opening of the thiadiazole ring may have inhibitory effects on MsEH. In fact these compounds are the precursors of their corresponding benzoylamino thiadiazole analogues, as shown below (Experimental).

Discussion

The mechanism of murine and human sEH inhibition by chalcone oxide derivatives has been analyzed in detail through both a kinetic approach and QSAR analysis.[35] The results of QSAR analyses of the substituent effects on the activity of chalcone congeners (**I**), having various phenyl substituents, demonstrated that the most sterically favorable moieties at the 4- and 4′-positions are *n*-pentyl (or phenyl) and *n*-propyl groups, respectively. Five bridge atoms (the α, β, and γ carbons as well as the carbons to either side) of chalcone oxide (**I**: R = R′ = H) were fitted to the -C-N-C-N-C- backbone of DCU (**35**). These two molecules superposed each other well, and the substituents (including H) at the 4- and 4′-positions extend to the sterically favorable fields (Fig. 4(a); the structure of chalcone oxide is not shown). However, the epoxide oxygen should correspond to the carbonyl carbon of DCU in this superposition according to our previous mechanistic model in which the nucleophilic attack by the COO- residue of Asp is performed at the α-carbon of the chalcone in the catalytic site.[35] Thus, the A-ring moiety of DCU probably corresponds to the left phenyl ring containing the 4-substituted R group of chalcone oxide.

The superposition of chalcone oxide (observed $pIC_{50} = 5.54$[35]) to DCU by overlapping the B-ring moiety of structure **II** on the benzoyl moiety as described above gives a similar prediction (calculated $pIC_{50} = 5.95$) to that obtained from the reversed overlapping in which the benzoyl moiety was superposed on the A-ring moiety (calculated $pIC_{50} = 4.98$), although the signs of deviations are different between them. In addition, as we reported previously, the hydrophobic moieties at the 4-position strengthened the inhibition, while neither electronic effects nor the hydrophobicity of the 4′-position appeared to influence the inhibitory activity.[9] Mullin and Hammock also determined that the inhibition is dominantly affected by hydrophobic terms and modulated by 4-position molecular refractivity and 4′-steric, but not electronic, parameters.[38] Hydrophobically favorable fields were found to encompass both A- and B-ring moieties as shown in Figure 4(c), which is partially consistent with the QSAR result for chalcone oxides. To make clear the overlapping between chalcone and DCU, the CoMFA analysis for the combined set of compounds including the chalcone oxide derivatives as well as other recently designed compounds is in progress.

The sterically unfavorable region encompassing the cyclohexyl moiety of DCU might be due to steric repulsion occurring between the inhibitor and amino acid residues in the active site which contain a benzene ring, such as Tyr381, Tyr465, or Trp334.[7] The hydrophobically unfavorable region surrounding the urea bridge may correspond to the region accommodating His523 and Asp 333. These amino acid residues contain imidazolidine and carboxylic groups which could potentially form hydrogen bonds with the inhibitor.

In addition to steric effects, hydrophobicity appears to be important as described above. This trend was evidenced by several things: the activity of siduron (**51**), which has

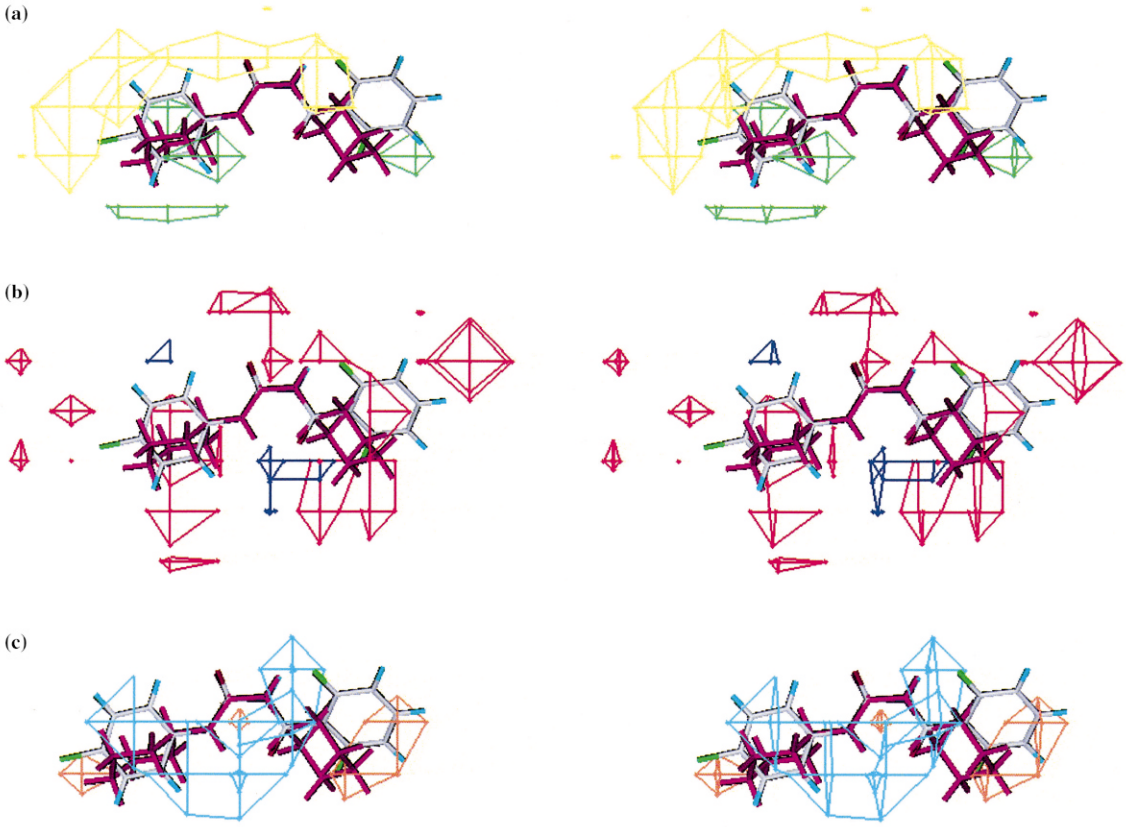

Figure 4. Stereoviews of CoMFA according to eqn (1) or eqn (5) with diflubenzuron (**18**) and DCU (**35**) colored with magenta. (a) The contours are shown to surround regions where a higher steric bulk increases (green) or decreases (yellow) the inhibition. (b) The contours are shown to surround regions where a positive (blue) and negative (red) electrostatic potential increases the inhibition. (c) The contours are shown to surround the regions where hydrophobic (orange) and hydrophilic (cyan blue) interactions increase the inhibition. The contour maps were drawn using the favored (80%) and disfavored (20%) contributions.

a CH_3 group on the cyclohexyl ring, was more potent than that of cyclohexylphenylurea (**16**). Additionally, the introduction of a CH_3 group on the benzene ring of cyclohexylphenylurea also resulted in increased activity, suggesting the importance of hydrophobic effects on the inhibition of sEH. However, the addition of molecular hydrophobicity (log*P*) did not significantly improve the correlation as shown in eqns (2) and (3) of Table 4. In QSAR studies examining enzyme inhibition and receptor binding, position-specific hydrophobicity is sometimes an important parameter not only for benzoylphenylureas,[36] but for some other compounds as well.[33] A prerequisite for the successful binding of a small molecule to a macromolecule, such as a receptor or enzyme, is a negative Gibbs free energy of binding. The target property to be correlated and predicted in a comparative analysis is a free energy value, and the Gibbs energy change (ΔG) depends on both the enthalpy change (ΔH) and the entropy change (ΔS).[33,37] Since the addition of the HINT term, not the molecular hydrophobicity log*P*, improved the correlation as shown in Table 4, the partial hydrophobic effects are probably related to the entropic contribution between a ligand molecule and a putative receptor. In fact, it was shown that an *N*-cyclohexyl group attached to a *trans*-amide structure packs well in the hydrophobic pocket and makes numerous van der Waals contacts with hydrophobic residues Val497, Phe406, Phe265, Trp524, and Tyr381.[7,8]

In eqn (5) (graphically shown in Figure 4(c)), the hydrophobic interaction at both the A- and B-ring moieties in structure **II** appears to be important. In eqns (4) and (5), 21 compounds were excluded from the set of compounds used to derive eqn (1), because HINT was unable to accurately calculate their log*P* values as listed in Tables 1–3. Another 3-D QSAR method, comparative similarity indices analysis (CoMSIA),[39] was also applied in an attempt to determine the hydrophobic effects for the total set of compounds ($n = 37$). However, the results with CoMSIA were not improved over those of CoMFA (data not shown). The poor prediction of compounds **4**–**9** and **41** is probably due to the fact that the hydrophobic factor was not considered in eqn (1). The predicted value ($pIC_{50} = 5.70$) of compound **41** by eqn (1) was 16 times higher than that ($pIC_{50} = 4.50$) predicted by eqn (5), suggesting that both position-specific steric and hydrophobic effects as well as electronic effects are important for activity. The prediction of activity for compounds **4**–**9** by eqn (5) appears to be meaningless due to the lack of confidence in the HINT log*P* values. The strength of the hydrophobic interactions has implications for the energetics of protein folding, substrate binding, and nucleic acid base stacking.[37]

The electronic effects of the 4-substituents of chalcone oxides (**I**) on the enzyme reaction rate were analyzed using a Hammet plot, in which σ^+ was applied, and the

coefficient of the sigma term in the correlation analysis was −0.66. This value indicates the development of a positive charge and excludes the formation of a true carbonium ion, being consistent with previous suggestions. Electrostatically negative fields are located above the carbonyl oxygen and a positive field is found beneath the carbonyl carbon atom of the urea, indicating that the electrostatically positive charge of the carbonyl carbon atom which is attacked by COO^- of Asp of MsEH is important to the activity.

The major steric, electrostatic, and hydrophobic interactions for the inhibition of sEH are summarized in Figure 5. As shown in Figures 4 and 5 the sterically favorable fields overlap the hydrophobically favorable fields, and electrostatically positive and negative fields are accommodated within the hydrophobically unfavorable fields. Hansch–Fujita type classical QSAR[40] studies would provide further understanding of the ligand–enzyme interactions surrounding the cyclohexyl groups. These studies are currently in progress. This will enable us to separate steric and hydrophobic effects as well as to distinguish electronic effects. By examining a series of cyclohexylurea congeners with various substituents in *o*-, *m*-, and *p*-positions we should be able to discern position-specific interactions.

In our recent study, the distribution of partial charge in the reaction coordinate of the opening of the epoxide ring was demonstrated by analyzing the X-ray structures of two alkylurea inhibitors, *N*-cyclohexyl-*N*′-decylurea (CDU) and *N*-cyclohexyl-*N*′-(4-iodophenyl)-urea (CIU), complexed with MsEH.[8] In these complexes, a constellation of hydrogen bonds that activate epoxide substrates for hydrolysis was observed, while it was not seen in the CPU-complex.[7] These inhibitors bind in the sEH active site and directly mimic the interactions consistent with the activation of a substrate epoxide ring for nucleophilic attack by Asp333. The urea carbonyl group accepts hydrogen bonds from Tyr465 and Tyr381. We demonstrated that these two tyrosine residues serve as general acid catalysts that activate the substrate epoxide ring for nucleophilic attack by Asp333. We explained that the activity of benzoylphenylureas was lowered by lowering the overall hydrophobicity compared to that of DCU. However, there must be an additional effect responsible for lowering the activity of benzoylphenylureas. We believe that the benzoyl carbonyl group is detrimental to the activity, even though weak activity can be observed sometimes. According to the 3-D structures, this carbonyl group may interfere with the nucleophilic attack of Asp333 at the urea carbonyl carbon. However, in the case of the chalcone oxide analogues, the carbonyl oxygen is "*cis*" to the epoxide oxygen, which enhances the inhibitory activity.[9]

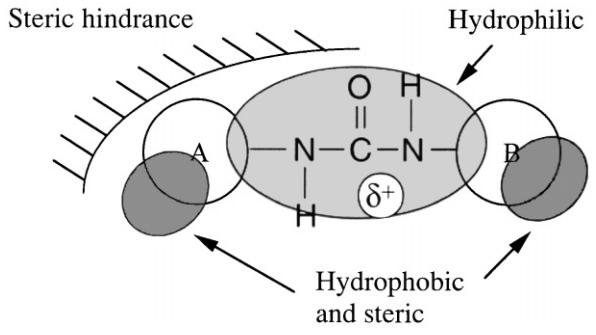

Figure 5. Summarized CoMFA–HINT map for the inhibition of sEH.

In this QSAR model only compound **39**, containing a thiourea structure, is not included in the analysis, even though three benzoyl thiourea analogues **13**–**15** were reasonably explained by this model. In order to further understand the favorable effect of thiourea, the synthesis of other thiourea analogues such as *N*-cyclohexyl-*N*′-phenylthiourea and *N*,*N*′-diphenylthiourea is in progress. The activity of industrial grade of diflubenzuron will also be included in the analysis as shown in Figure 3. However, we have to account for the potential existence of impurities in commercially acquired samples, since the presence of trace contaminants can strongly affect enzyme activity. For example, the presence of even 1% of DCU in the industrial batch of diflubenzuron could explain the noted inhibitory activity ($pIC_{50} = 4.57$), whereas synthetically prepared pure diflubenzuron was inactive. Based on this 3-D-QSAR model new sEH inhibitors are being designed, and their synthesis and bioassay are in progress.

The application of this model to the rational design of new inhibitors gives us several new insights. Since the substrate binding is governed mostly by van der Waals contacts made with the residues defining the active site, one strategy would be to maximize the number of available associations. This observation is supported by the large sterically and hydrophobically favored fields surrounding the inhibitors (Fig. 4(a) and (c)). We have synthesized diadamantylurea, which also exhibited high activity (unpublished data). Therefore new classes of inhibitors should explore the limits of steric bulk for favorable activity. The other major site of activity is the negative potential field around the NH groups of the urea and carbonyl oxygen. The necessity of at least one NH group has been well established. However, moieties which increased the negative potential around these groups could lead to increased activity. Along the same theme, maximizing the electronic charge of the carbonyl carbon is important for the activity.

Other effects of benzoylphenylureas on mammalian systems such as stimulation of hematopoesis,[25] antitumor activity in vivo against P388 and L1210 leukemias,[21,22] and inhibition of tubulin polymerization and HL-60 cell growth[23,24] may be related to the inhibition of sEH, and the mode of action for the inhibition of chitin synthesis.

Conclusion

Among 271 insect growth regulators tested, 18 benzoylphenylureas were active against MsEH. However, these compounds were very weak when compared with several other ureas, such as DCU and urea-containing

herbicides. In the CoMFA results, large sterically unfavorable fields were concentrated above the A-ring and the urea bridge moiety, and sterically favorable fields were mainly found beneath the A- and B-rings. A series of negative potential fields surrounds the whole molecule and one large positive potential field is located beneath the carbonyl carbon atom. In this CoMFA model, only one compound which contained a thione (C=S) instead of a carbonyl (C=O) group was excluded. The ligand binding modes visualized were consistent with the results obtained from crystallographic analysis. The 3-D QSAR analysis for an expanded set of compounds including thioureas, carbamates, and alkyl amines (unpublished data) will enable us to more precisely map the ligand–receptor environment. This 3-D QSAR model will be useful for further probing the active site and mechanism of sEH. In addition, it will be a valuable tool for designing the rational synthesis of new potent sEH inhibitors.

Experimental

Bioassay

Inhibition of sEH was reported as the IC_{50} (concentration of inhibitor which results in 50% inhibition of the enzyme) according to previous methods.[9] Briefly, recombinant mouse sEH, expressed in our baculovirus system,[28,29] was purified from cell lysate by affinity chromatography[41] and the purity (> 97% pure) of each protein was judged by SDS–PAGE. The IC_{50} determinations for each inhibitor employed a spectrophotometric assay using racemic 4-nitrophenyl-*trans*-2,3-epoxy-3-phenylpropyl carbonate as the substrate in a polystyrene 96-well microtiter plate.[42] In each well, 20 μL of enzyme preparation, 2 μL of inhibitor solution in DMF (0.05 to 500 μM), and 180 μL of sodium phosphate buffer (0.1M, pH 7.4) containing 0.1 mg/mL of BSA were combined. This mixture was incubated at 30 °C for 5 min, allowing for maximal inhibition with little enzyme reactivation, followed by addition of 4 μL of a 2 mM solution of substrate. Activity was assessed by measuring the appearance of the 4-nitrophenolate anion at 405 nm at 30 °C after 1 min (Spectramax 200; Molecular Device, Inc., Sunnyvale, CA). All assays were performed in quadruplicate, and the IC_{50} was determined by regressions of at least five datum points for each analysis with a minimum of two points in the linear region of the curve on either side of the IC_{50}. Each curve was generated from at least three separate runs. In at least one run, compounds of a similar potency were included to ensure rank order. The reciprocal logarithm value of IC_{50}, pIC_{50}, was used as the activity index.

Chemicals

Compounds (**1**, **2**, **4**, **6**, **8**) were prepared from the corresponding aniline (1.4–4.7 mmol) and an excess amount of benzoyl isocyanate by mixing them in tetrahydrofuran (THF) at room temperature followed by recrystallization of the insoluble products from 95% ethanol. Benzoyl isocyanate was prepared by refluxing benzamide (3 g, 24.7 mmol) and oxalyl chloride (5.77 g, 45 mmol) for 3 h in dichloroethane (10 mL), and purified by distillation (65 °C at 1 mm Hg). Compounds (**3**, **5**, **7**, **9**) were also obtained from the corresponding anilines and 4-chlorobenzoyl isocyanate in a similar manner as above. 4-Chlorobenzoyl isocyanate was prepared by refluxing 4-chlorobenzamide (2.0 g, 12.9 mmol) and oxalyl chloride (2.02 g, 15.9 mmol) for 1.5 h in dichloroethane (10 mL) and purified by distillation (100 °C at 5 mmHg). Since benzoyl isocyanate and 4-chlorobenzoyl isocyanate are unstable, they were used immediately for the following reactions without determining the yield. All products were recrystallized from ethanol. Yields for compounds **1**–**9** ranged from 30 to 70%, and these and all other yields were not optimized.

Compounds **10** and **11** were prepared from phenyl isocyanate (0.75 g, 6.3 mmol) and *p*-chlorophenyl isocyanate (0.58 g, 3.8 mmol) by refluxing with benzylamine in THF (10 mL) followed by recrystallization of the insoluble products from 95% ethanol. Yields were 23% (**10**) and 51% (**11**).

Dibenzylurea (**12**) was prepared from benzylamine (0.86 g, 7.98 mmol) and 1,1-carbonyldiimidazole (1.09 g, 6.72 mmol). After stirring benzylamine and 1,1-carbonyldiimidazole in 95% aqueous ethanol at room temperature overnight, the reaction afforded colorless needles (0.18 g, 18.8%) without recrystallization. mp 168.5–169.5 °C.

1-(4-Chlorophenyl)-3-(2-fluorobenzoyl)thiourea (**13**): 2-fluorobenzoyl chloride (1.85 g, 11.7 mmol) was added dropwise to the ammonium thiocyanate (0.98 g, 12.9 mmol) in anhydrous acetone (7 mL) with stirring, then refluxed for 5 min. 4-Chloroaniline (1.85 g, 14.5 mmol) in 3.5 mL of acetone was added to the reaction mixture followed by an additional 5 min of refluxing. The mixture was then poured into water, resultant crystals were collected by filtration and recrystallized from ethanol to yield 2.02 g (56%). Mp 130–131 °C.

Compounds **14** and **15** were synthesized from the appropriate benzoyl isothiocyanates and corresponding 4-substituted benzoyl hydrazines. Benzoyl isothiocyanate was prepared from the benzoyl chloride and either ammonium thiocyanate (NH_4SCN) or potassium thiocyanate (KSCN) according to the conventional method.[43] 2,6-Dimethoxybenzoyl chloride (2.52 g, 12.6 mmol) dissolved in acetone was added dropwise to KSCN (4.5 g, 22.3 mmol) dissolved in dry benzene (10 mL). The mixture was stirred at room temperature until the color changed to reddish yellow, then refluxed for 5 min. After cooling, KCl was removed by filtration. The filtrate was purified by distillation (139 °C at 17 mmHg) to afford 2,6-dimethoxybenzoyl isothiocyanate (1.27 g) in a yield of 45%. A mixture of 4-iodobenzoic acid (12.4 g, 50.0 mmol), ethanol (2.9 mL), and sulfuric acid (0.9 mL) in dichloromethane (15 mL) was refluxed for 10 h. After washing the dichloromethane layer with water, 5% $NaHCO_3$, and water, successively, it was dried over anhydrous sodium sulfate. Ethyl 4-iodobenzoate was obtained by distillation (133 °C, 8 mmHg). Yield was 10.22 g (78%). Ethyl 4-iodobenzoate (10.22 g),

60% hydrazinehydrate (1.85 g), and ethanol (10 mL) were mixed, then refluxed for 8 h. After evaporating the ethanol, the residue was washed with ice-cold water followed by recrystallization from ethanol to obtain 4-iodobenzoylhydrazine (4.37 g, 45.1%). 2,6-Dimethoxybenzoyl isothiocyanate (2.11 g) and 4-ethyl benzoate (2.48 g) were dissolved in benzene (20 mL) and refluxed for 2 h. After evaporating the solvent, the residue was washed with a minimal amount of diethyl ether and water. Recrystallization was performed from ethanol to afford 2,6-dimethoxybenzoyl-4-iodobenzoylthiosemicarbazide (**15**; 0.71 g; 69%). Mp 185–186 °C. The corresponding 4-nitro analogue (**14**) was synthesized in a similar manner as above.

Compound **17** was obtained as a colorless crystalline solid in 81% yield from the slow addition of cyclohexyl isocyanate (0.63 g, 5.0 mmol) to a vigorously stirred solution of *p*-toluidine (0.54 g, 5.0 mmol) in 10 mL of hexane, and compound **16** was prepared from the corresponding aniline as well. Each structure was characterized by 300 MHz or 500 MHz ^{1}H NMR spectra recorded on the Bruker AC-300 or ARX-500 and elemental analyses. The analytical values for C, H and N agreed with calculated

Table 5. Physical data for all newly synthesized compounds

No.[a]	Melting point (°C)	Elemental analyses (%)	^{1}H NMR ($CDCl_3$)[b] (ppm)
1	201–202	Found: C-72.95, H-6.80, N-9.45 Calcd: C-73.08, H-6.85, N-9.51	1.34 (s, 9H, *t*-Bu), 7.36–8.04(m, ArH), 9.41 (s, 1H, NH), 10.84 (s, 1H, NH)
2	206–207	Found: C-72.28, H-4.85, N-8.43 Calcd: C-72.16, H-4.74, N-8.45	7.00–8.02 (m, 14H, ArH), 9.34 (br, 1H, NH), 10.80 (s, 1H, NH)
3	219–220	Found: C-65.49, H-4.12, N-7.64 Calcd: C-65.49, H-4.00, N-7.61	6.98–7.94 (m, 13H, ArH), 9.41 (s, 1H, NH), 10.76 (s, 1H, NH)
4	160–161	Found: C-68.27, H-7.37, N-11.37 Calcd: C-68.28, H-7.30, N-11.27	1.24–2.00 (m, 10H, cHexH), 3.74–3.85 (m, 1H, -N-cHexH[c]), 7.47–7.92 (m, 5H, ArH), 8.63 (d, 1H, J = 7.2 Hz, NH), 8.84 (br, 1H, NH)
5	222.0–222.5	Found: C-59.89, H-6.10, N-9.98 Calcd.: C-60.15, H-6.06, N-9.99	1.26–1.99 (m, 10H, cHexH), 3.70–3.80 (m, 1H, -N-cHexH[c]), 7.43–7.93 (m, 4H, ArH), 8.64 (d, 1H, J = 7.5 Hz, NH), 9.39 (s, 1H, NH)
6	176.5–177.5	Found: C-72.69, H-9.15, N-8.48 Calcd: C-72.54, H-9.19, N-8.50	1.26–1.74 (m, 22H, cDodH), 4.00–4.04 (m, 1H, -N-cDodH[d]) 7.50–7.88 (m, 5H, ArH), 8.52–8.57 (m, 2H, 2 × NH)
7	207–208	Found: C-65.83, H-8.01, N-7.68 Calcd: C-65.85, H-8.13, N-7.80	1.25–1.71 (m, 22H, cDodH), 3.96–4.07 (m, 1H, -N-cDodH[d]) 7.44–7.95 (m, 4H, ArH), 8.65 (d, 1H, J = 8.0 Hz, NH), 9.63 (s, 1H, NH)
8	166–167	Found: C-70.85, H-5.55, N-11.02 Calcd: C-70.92, H-5.60, N-11.02	4.57 (d, 2H, J = 5.9, CH_2), 7.27–7.93 (m, 10H), 9.10 (br, 1H, NH), 9.20 (br, 1H, NH)
9	199–200	Found: C-62.40, H-4.54, N-9.70 Calcd: C-62.37, H-4.45, N-9.71	4.57 (d, 2H, J = 5.9 Hz, CH_2), 7.27–7.92 (m, 9H, ArH), 9.12 (br, 1H, NH), 9.67 (s, 1H, NH)
10	168–169	Found: C-74.31, H-6.24, N-12.38 Calcd: C-74.23, H-6.19, N-12.64	4.42 (d, 2H, J = 5.8), 5.18 (br, 1H, NH), 6.50 (s, 1H, NH), 7.05–7.34 (m, 10H, ArH)
11	206	Found: C-64.50, H-5.03, N-10.74 Calcd: C-64.35, H-4.85, N-11.02	4.42 (d, 2H, J = 5.8), 6.13 (br, 1H, NH), 7.17–7.39 (m, 9H, ArH), 8.01 (s, 1H, NH)
12	168.5–169.5	Found: C-74.97, H-6.71, N-11.66 Calcd: C-75.09, H-6.69, N-11.73	4.38 (d, 4H, J = 5.8 Hz, CH_2), 4.64 (br, 2H, 2×NH), 7.26–7.32 (m, 10H, ArH)
13	123–125	Found: C-54.55, H-3.38, N-9.09 Calcd: C-3.26, H-54.46, N-9.07	7.23–8.12 (m, 8H, Ar), 9.67 (d, 1H, J = 14.6, CS-NH-Ar), 12.55 (s, 1H, CO-NH-CS-)
14	198–200	Found: C-50.60, H-3.98, N-13.79 Calcd: C-50.49, H-3.99, N-13.85	3.89 (s, 6H, 2×OCH_3), 6.61–8.38 (m, 7H, Ar), 8.92 (s, 1H, NH), 10.09 (d, J = 6.6 Hz, NH), 13.38 (d, 1H, J = 8.0 Hz, NH)
15	185–186	Found: C-42.12, H-3.24, N-8.62 Calcd: C-42.07, H-3.32, N-8.66	3.87 (s, 6H, 2×OCH_3), 6.59–7.87 (m, 7H, ArH), 8.84 (s, 1H, NH), 9.96 (d, J = 7.2 Hz, NH), 13.33 (d, 1H, J = 6.8 Hz, NH)
16	183.5–184.5	Found: C-71.33, H-8.46, N-12.79 Calcd: C-71.53, H-8.31, N-12.83	1.09–1.99 (m, 10H, cHexH), 3.60–3.73 (m, 1H, N-cHexH[c]), 4.57 (br, 1H, NH), 6.16 (s, 1H, NH), 7.07–7.34 (m, 5H, ArH)
17	203–204	Found: C-72.60, H-8.56, N-12.00 Calcd: C-72.38, H-8.68, N-12.06	1.03–1.98 (m, 10H, cHexH), 2.32 (s, 3H, CH_3), 3.60–3.72 (m, 1H, N-cHexH[c]),4.55 (d, 1H, J = 7.6 Hz, NH), 6.09 (s, 1H, NH), 7.13 (s, 4H, ArH),

[a]Numbers correspond to those in Table 1.
[b]If compounds were insoluble in $CDCl_3$, a drop of DMSO-d_6 was added, and ^{1}H NMR was recorded at 300 MHz. For compounds **14** and **15** it is recorded at 500 MHz.
[c]-N-cHexH means the CH-proton of cyclohexyl group attached to N atom.
[d]-N-cDodH means the CH-proton of cyclododecyl group attached to N atom.

values within an error of ±0.3%. All compounds synthesized are listed in Table 1. Melting points, NMR spectral data, and elemental analyses are summarized in Table 5.

A hundred and eighty-one benzoylphenylureas (**III** in Figure 1) having various substituents at both benzene rings[36,44–47] and sixteen benzoylaminothiadiazole analogues[34] with various substituents at both benzene rings were taken from our stock samples prepared in our previous studies. The benzoylphenylureas included 114 2,6-difluorobenzoylurea analogues with single- or multiply-substituted phenyl moieties (Y_n), 34 2,6-dichlorobenzoylurea analogues (**III**; $X_n = 2,6\text{-}Cl_2$) with single- or di-substituted phenyl moieties (Y_n), and 33 4-chlorophenylurea appendages with various *N*-substituted benzoyl moieties. Compounds **34**–**50** were previously reported,[9] and the data of compounds **51** and **52** as well.[13]

Acknowledgements

We thank the following sources for funding: NIEHS ES02710, NIEHS Superfund Basic Research Program ES04699, UC Systemwide Ecotoxicology Training Program, U.S. EPA Center for Ecological Health Research CR819658, and the NIEHS Center for Environmental Health Sciences ES05707.

References

1. Oesch, F. *Xenobiotica* **1973**, *3*, 305.
2. Ota, K.; Hammock, B. D. *Science* **1980**, *207*, 1479.
3. Wixtrom, R. N.; Hammock, B. D. In *Biochemical Pharmacology and Toxicology*; Zakim, D., Vessey, D. A., Eds.; Wiley: New York, 1985; Vol. 1, pp 1–93.
4. von Dippe, P.; Amoui, M.; Alves, C.; Levy, D. *Am. J. Physiol.* **1993**, *264*, G528.
5. von Dippe, P.; Amoui, M.; Stellwagen, R. H.; Levy, D. *J. Biol. Chem.* **1996**, *271*, 18176.
6. Moghaddam, M. F.; Grant, D. F.; Cheek, J. M.; Greene, J. F.; Williamson, K. C.; Hammock, B. D. *Nat. Med.* **1997**, *3*, 562.
7. Argiriadi, M. A.; Morisseau, C.; Hammock, B. D.; Christianson, D. W. *Proc. Natl. Acad. Sci. USA* **1999**, *96*, 10637.
8. Argiriadi, M. A.; Morisseau, C.; Goodrow, M. H.; Dowdy, D. L.; Hammock, B. D.; Christianson, D. W. *J. Biol. Chem.* **2000**, *275*, 15265.
9. Morisseau, C.; Goodrow, M. H.; Dowdy, D.; Zheng, J.; Greene, J. F.; Sanborn, J. R.; Hammock, B. D. *Proc. Natl. Acad. Sci. USA* **1999**, *96*, 8849.
10. Newman, J. W., Denton, D. L., Morisseau, C., Koger, C. S., Wheelock, C. E., Hinton, D. E., Hammock, B. D. submitted to *Environmental Health Perspective*.
11. Marks, E. P., Leighton, T., Leighton, F. In *Insecticide Mode of Action*; Coats, J. R., Ed.; Academic Press: New York, 1982, pp 281–313.
12. Cohen, E.; Casida, J. E. *Pestic. Biochem. Physiol.* **1980**, *13*, 129.
13. Mitsui, T.; Nobusawa, C.; Fukami, J. *J. Pestic. Sci.* **1981**, *6*, 155.
14. Nakagawa, Y.; Matsumura, F. *Insect Biochem. Molec. Biol.* **1994**, *24*, 1009.
15. Ishii, S.; Matsumura, F. *Insect Biochem. Molec. Biol.* **1992**, *22*, 69.
16. Nakagawa, Y.; Ishii, S.; Matsumura, F. *Insect Biochem. Molec. Biol.* **1996**, *26*, 891.
17. Horst, M. *J. Biol. Chem.* **1981**, *256*, 1412.
18. Leighton, T.; Marks, E. P.; Leighton, F. *Science* **1981**, *213*, 905.
19. Oberlander, H., Silhacek, D. L. In *Insecticides with Novel Mode of Action*; Ishaaya, I., Degheele, D., Eds.; Springer: Berlin, 1998, pp 92–105.
20. Nakagawa, Y. *J. Pestic. Sci.* **1996**, *21*, 460 (in Japanese).
21. Nakajima, T.; Masuda, H.; Okamoto, T.; Watanabe, M.; Yokoyama, K.; Yamada, N.; Fujimoto, S.; Tsukagoshi, S.; Taguchi, T. *Cancer Chemother. Pharmacol.* **1991**, *28*, 351.
22. Okada, H.; Koyanagi, T.; Yamada, N.; Haga, T. *Chem. Pharm. Bull.* **1991**, *39*, 2308.
23. Paull, K. D.; Lin, C. M.; Malspeis, L.; Hamel, E. *Cancer Research* **1992**, *52*, 3892.
24. Ando, N.; Nakajima, T.; Masuda, H.; Kawabata, Y.; Iwai, M.; Watanabe, M.; Kagitani, Y.; Yamada, N.; Tsukagoshi, S. *Cancer Chemother. Pharmacol.* **1995**, *37*, 63.
25. Jenkins, V. K. **1992**, US Patent 5166180.
26. Cramer, R. D. III; Patterson, D. E.; Bunce, J. D. *J. Am. Chem. Soc.* **1988**, *110*, 5959.
27. Kellogg, G. E.; Semus, S. F.; Abraham, D. J. *J. Comp.-Aided Mol. Design* **1991**, *5*, 545.
28. Grant, D. F.; Storms, D. H.; Hammock, B. D. *J. Biol. Chem.* **1993**, *268*, 17628.
29. Beetham, J. K.; Tian, T.; Hammock, B. D. *Arch. Biochem. Biophys.* **1993**, *305*, 197.
30. Cruse, W. B. T. *Acta Cryst.* **1978**, *B34*, 2904.
31. Baroni, M.; Costantino, G.; Cruciani, G.; Riganelli, D.; Valigi, R.; Clementi, S. *Quant. Struct.-Act. Rel.* **1993**, *12*, 9.
32. Leo, A. *Chem. Rev.* **1993**, *93*, 1281.
33. Hansch, C.; Leo, A. *Exploring QSAR: Fundamentals and Applications in Chemistry and Biology*. American Chemical Society: Washington, DC, 1995.
34. Nakagawa, Y.; Nishimura, K.; Izumi, K.; Kinoshita, K.; Kimura, K.; Kurihara, N.; Fujita, T. *J. Pestic. Sci.* **1996**, *21*, 195.
35. Morisseau, C.; Du, G.; Newman, J. W.; Hammock, B. D. *Arch. Biochem. Biophys.* **1998**, *356*, 214.
36. Nakagawa, Y.; Izumi, K.; Oikawa, N.; Kurozumi, A.; Iwamura, H.; Fujita, T. *Pestic. Biochem. Physiol.* **1991**, *40*, 12.
37. Sharp, K. A.; Nicholls, A.; Friedman, R.; Honig, B. *Biochemistry* **1991**, *30*, 9686.
38. Mullin, C. A.; Hammock, B. D. *Arch. Biochem. Biophys.* **1982**, *216*, 423.
39. Klebe, G.; Abraham, U.; Mietzner, T. *J. Med. Chem.* **1994**, *37*, 4130.
40. Hansch, C.; Fujita, T. *J. Am. Chem. Soc.* **1964**, *86*, 1616.
41. Wixtrom, R. N.; Silva, M. H.; Hammock, B. D. *Anal. Biochem.* **1988**, *169*, 71.
42. Dietze, E. C.; Kuwano, E.; Hammock, B. D. *Anal. Biochem.* **1994**, *216*, 176.
43. Douglass, I. B.; Dains, F. B. *J. Am. Chem. Soc.* **1934**, *56*, 719.
44. Nakagawa, Y.; Kitahara, K.; Nishioka, T.; Iwamura, H.; Fujita, T. *Pestic. Biochem. Physiol.* **1984**, *21*, 309.
45. Nakagawa, Y.; Iwamura, I.; Fujita, T. *Pestic. Biochem. Physiol.* **1985**, *23*, 7.
46. Nakagawa, Y.; Sotomatsu, T.; Irie, K.; Kitahara, K.; Iwamura, H.; Fujita, T. *Pestic. Biochem. Physiol.* **1987**, *27*, 143.
47. Nakagawa, Y.; Akagi, T.; Iwamura, H.; Fujita, T. *Pestic. Biochem. Physiol.* **1988**, *30*, 67.
48. Sotomatsu, T.; Nakagawa, Y.; Fujita, T. *Pestic. Biochem. Physiol.* **1987**, *27*, 156.
49. Nakagawa, Y.; Izumi, K.; Oikawa, N.; Sotomatsu, T.; Shigemura, M.; Fujita, T. *Environ. Toxicol. Chem.* **1992**, *11*, 901.
50. Sotomatsu, T.; Shigemura, M.; Murata, Y.; Fujita, T. *J. Pharm. Sci.* **1993**, *82*, 776.